

## Research Paper

# Anti-cancer Activity of Novel TM4SF5-Targeting Antibodies through TM4SF5 Neutralization and Immune Cell-Mediated Cytotoxicity

Hye-Mi Ahn<sup>1</sup>, Jihye Ryu<sup>2</sup>, Jin Myeong Song<sup>3</sup>, Yunhee Lee<sup>1</sup>, Hye-Jin Kim<sup>2</sup>, Dongjoon Ko<sup>1,4</sup>, Inpyo Choi<sup>1</sup>, Sang Jick Kim<sup>3</sup>✉, Jung Weon Lee<sup>2</sup>✉, Semi Kim<sup>1,4</sup>✉

1. Immunotherapy Convergence Research Center, Korea Research Institute of Bioscience and Biotechnology, Daejeon, Korea;
2. Department of Pharmacy, College of Pharmacy, Seoul National University, Seoul, Korea;
3. Biochemicals & Synthetic Biology Research Center, Korea Research Institute of Bioscience and Biotechnology, Daejeon, Korea;
4. Department of Functional Genomics, Korea University of Science and Technology, Daejeon, Korea.

✉ Corresponding authors: Semi Kim, Ph.D. Immunotherapy Convergence Research Center, Korea Research Institute of Bioscience and Biotechnology, 125 Gwahak-ro, Yuseong-gu, Daejeon 34141, Korea E-mail: semikim@kribb.re.kr; Tel: +82-42-860-4228. Or Jung Weon Lee, Ph.D. Department of Pharmacy, College of Pharmacy, Seoul National University, 1 Gwanak-ro, Gwanak-Gu, Seoul 08826, Korea E-mail: jwl@snu.ac.kr; Tel: +82-2-880-2495. Or Sang Jick Kim, Ph.D. Biochemicals & Synthetic Biology Research Center, Korea Research Institute of Bioscience and Biotechnology, 125 Gwahak-ro, Yuseong-gu, Daejeon 34141, Korea E-mail: sjick@kribb.re.kr; Tel: +82-42-860-4229.

© Ivyspring International Publisher. This is an open access article distributed under the terms of the Creative Commons Attribution (CC BY-NC) license (<https://creativecommons.org/licenses/by-nc/4.0/>). See <http://ivyspring.com/terms> for full terms and conditions.

Received: 2016.03.23; Accepted: 2016.08.04; Published: 2017.01.11

## Abstract

The transmembrane four L6 family member 5 (TM4SF5) protein is a novel molecular target for the prevention and treatment of hepatocellular carcinoma. TM4SF5 is highly expressed in liver, colon, esophageal, and pancreatic cancers and is implicated in tumor progression. Here, we screened monoclonal antibodies that specifically bound to the extracellular loop 2 (EC2) of TM4SF5 from a phage-displayed murine antibody (single-chain variable fragment; scFv) library. We constructed and characterized chimeric antibodies, Ab27 and Ab79, of scFv fused with Fc domain of human IgG1. The affinity ( $K_D$ ) of Ab27 and Ab79 for soluble EC2 was approximately 9.2 nM and 16.9 nM, respectively, as determined by surface plasmon resonance analysis. Ab27 and Ab79 efficiently bound to native TM4SF5 on the cell surface were internalized into the cancer cells, leading to a decrease in cell surface TM4SF5. Ab27 and Ab79 inhibited the proliferation and invasion of TM4SF5-positive liver and colon cancer cells and reduced FAK and c-Src phosphorylation. Ab27 and Ab79 also enhanced anoikis sensitivity and reduced survivin. Ab27 mediated antibody-dependent cell-mediated cytotoxicity *in vitro*. Ab27 and Ab79 efficiently inhibited tumor growth in a liver cancer xenograft model. These results strongly support the further development of Ab27 as a novel anti-cancer agent in the clinic.

Key words: TM4SF5, antibody, therapeutics, liver cancer, colon cancer, phage display.

## Introduction

Hepatocellular carcinoma (HCC), the most common type of liver cancer, is the third most common cause of cancer-related deaths worldwide [1, 2]. The prognosis of HCC is poor due to the difficulty of early diagnosis and lack of effective systemic therapies for advanced disease. HCC is frequently resistant or refractory to conventional chemotherapy and radiotherapy. The high frequency of recurrence and liver function failure after surgical resection also

contribute to the poor survival rate [2]. Colorectal cancer is the most common cancer and its incidence and mortality rates are increasing worldwide [3]. The prognosis for most colon cancer patients is still poor despite advances in treatment options, such as the use of angiogenesis inhibitors (e.g., bevacizumab) and EGFR-targeting antibodies (e.g., cetuximab) for treatment of metastatic colorectal cancer in the past decade [3]. There remains, therefore, an urgent unmet

need for effective therapies for liver and colorectal cancer patients.

Tetraspanins, also known as the transmembrane 4 superfamily (TM4SF), contain four transmembrane domains, two extracellular loops, one intracellular loop, and the N- and C-terminal tails [4]. Expressed on the cell surface, these molecules interact/crosstalk with other TM4SFs, integrins, and/or growth factor receptors to form massive protein-protein complexes [5]. These mediate intracellular signaling to regulate cell differentiation, activation, growth, and migration [6]. TM4SF5, highly expressed in a number of diverse cancers, including liver, colon, pancreatic, and esophageal cancers [7-9], is implicated in tumor development and progression. We previously reported that TM4SF5 plays a critical role in HCC development and metastasis; TM4SF5 mediates epithelial-mesenchymal transition (EMT), proliferation, and angiogenesis [8, 10] and also promotes self-renewal and other properties of circulating tumor cells via its interaction with CD44 [11]. TM4SF5 associates with the integrins  $\alpha 2$ ,  $\alpha 5$ , and  $\beta 1$ , and epidermal growth factor receptor (EGFR), to mediate cell migration, tumorigenesis, and drug resistance [10, 12]. The interaction of TM4SF5 with integrin  $\alpha 2\beta 1$  [13], EGFR [12], or CD44 [11] probably occurs via the extracellular loop 2 (EC2). Blocking the EC2 domain using an anti-TM4SF5 compound, such as synthetic chalcone derivative (TSAHC), or by introducing point mutations at N-glycosylation residues within the EC2, inhibits TM4SF5-mediated growth and loss of contact inhibition, as well as invasion of tumor cells [14], thus highlighting a critical role for the EC2 domain in TM4SF5-mediated functions. These reports suggest that TM4SF5 may serve as a molecular target for anti-cancer therapy and that a TM4SF5-specific monoclonal antibody may have potential as a therapeutic agent for the treatment of cancer.

In this study, we screened a mouse single-chain variable fragment (scFv) library and identified novel monoclonal antibodies specific for the EC2 domain of human TM4SF5, which were then used to generate the scFv-human Fc chimeric antibodies Ab27 and Ab79. We then explored the therapeutic potential of Ab27 and Ab79 against TM4SF5-expressing liver and colon cancer cells and also evaluated their mechanisms of anti-tumor activity. Our results demonstrated that antibody Ab27 inhibited cancer cell invasion and proliferation and reduced tumor growth through TM4SF5 neutralization. Ab27 also exhibited an immune cell-mediated cell killing activity. The further development of Ab27 as an anti-cancer agent is warranted.

## Materials and Methods

### Expression and purification of antigen

A cDNA fragment encoding the human TM4SF5 EC2 domain (GenBank accession number NM\_003963) was subcloned into the *pCMV-Fc-myc* vector [15] that was constructed by inserting a leader sequence (GenBank accession number M19901) and Fc and myc tags into the *HindIII-XhoI* sites of the *pcDNA3(oriP)-FcγRI* vector [16]. The resulting recombinant EC2-Fc fusion protein expression plasmid encoding the TM4SF5 EC2 (amino acid residues 113-157) fused to the Fc of human immunoglobulin IgG1 was transfected into HEK293E cells using Lipofectamine 2000 (Invitrogen, Carlsbad, CA, USA). At 48 h after transfection, the medium was changed to serum-free medium. Conditioned medium was collected at intervals of 2 to 3 days. The conditioned medium was subjected to affinity chromatography on a Protein A excellose column (Bioprogen, Daejeon, Korea) to obtain purified EC2-Fc fusion protein.

### Library panning and screening

A phage-displayed mouse antibody (scFv format) library constructed using the phagemid vector, *pDR-D1* [17] was used to select clones recognizing TM4SF5. The library phages were subjected to two rounds of panning against the recombinant EC2-Fc protein. Immunoplate wells (Nunc, Naperville, IL, USA) were coated overnight at 4°C with either 200 ng of EC2-Fc or human IgG (Sigma, St Louis, MO, USA), and blocked with 4% skim milk in PBS (10 mM phosphate/150 mM NaCl, pH 7.4) for 2 h at 37°C. Approximately  $10^{12}$  colony-forming unit of phage particles were preincubated in the human IgG-coated wells for 30 min at 37°C to remove Fc-specific binders. The subtracted phages were then incubated in the EC2-Fc-coated wells for 2 h at 37°C. The wells were washed with 0.05% Tween 20 in PBS (PBST; five times for round one, and ten times for round two), and bound phages were eluted with 0.1 M glycine-HCl (pH 2.2) and neutralized with 2 M Tris base. The eluted phages were amplified by infecting ER2738 cells followed by super-infection with the VCSM13 helper phage (Stratagene, La Jolla, CA, USA), before being used for the next panning round.

Ninety-six colonies were randomly selected from the output plate after the second round of panning to screen for individual scFv phage clones that specifically recognized EC2-Fc. The scFv phage clones were grown until the OD reached 0.5 and then rescued by super-infection with helper phages. The rescued phages were applied onto the EC2-Fc or human IgG-coated microwells. The phage binding

was detected by phage ELISA using horseradish peroxidase (HRP)-conjugated anti-M13 antibody (GE healthcare, Uppsala, Sweden). The clones showing TM4SF5-specific binding were subjected to DNA sequencing, and the nucleotide sequences determined were submitted to IMG/IT/V-QUEST (<http://imgt.cines.fr/vquest>) for sequence analysis. Ten different clones were selected and used for further analysis.

### Phage ELISA

Microtiter wells were coated with EC2-Fc or human IgG diluted in 50 mM sodium carbonate buffer (pH 9.6) at 4°C overnight and blocked with 2% BSA in PBS. The plates were washed four times in PBST between the different steps. All incubations were carried out at 37°C for 1 to 2 h. HRP-conjugated goat anti-M13 (GE healthcare) was used for the detection of any bound phage. Color was developed using the 3,3',5,5'-tetramethylbenzidine (TMB) chromogenic substrate reagent set (BD Biosciences, San Diego, CA, USA), and the absorbance was measured at 450 nm using a microtiter reader (Emax, Molecular Devices, Sunnyvale, CA, USA).

### Construction and purification of scFv-hFc

The scFv inserts were cut out of the phagemid DNA using SfiI-digestion and cloned directly into the pDR-OriP-Fc1 mammalian expression vector as described previously [17]. The classical (G<sub>4</sub>S)<sub>3</sub> sequence (GGGGSGGGSGGGGS) was used as a linker between the variable heavy and light chains. The resulting scFv-Fc expression plasmid was transfected into HEK293E cells, and purification of the scFv-Fc protein was performed in a manner similar to that used for the EC2-Fc fusion protein. Recombinant Fc proteins produced from the empty *pCMV-Fc-myc* vector or HA6, a scFv-Fc recognizing the hepatitis A virus (HAV) [17], were used as negative controls.

### Cell cultures

Human embryonic kidney 293E (HEK293E), SW480, HCT-116, HT-29, LoVo, LS174T, Colo205 (colon cancer), PC3 (prostate cancer), and the CD16-expressing NK-92 (interleukin (IL)-2-dependent Natural Killer (NK)) cell lines were purchased from the American Type Culture Collection (ATCC; Manassas, VA, USA). The SNU-398 liver cancer cell line was purchased from the Korean Cell Line Bank (KCLB; Seoul, Korea). HEK293E and LS174T cells were maintained in DMEM with 10% fetal bovine serum (FBS) at 37°C in 5% CO<sub>2</sub>. The SW480, HCT-116, HT-29, LoVo, Colo205, PC3, and SNU-398 cells were maintained in RPMI1640 with 10% FBS at 37°C in 5% CO<sub>2</sub>. The stable SNU449Cp (TM4SF5-low), SNU449Tp and SNU449T<sub>7</sub> (both highly TM4SF5-positive) liver

cancer transfectant cell lines and parental SNU449 cells were maintained as previously described [8]. CD16-expressing NK-92 cells were maintained in A-MEM with 12.5% FBS, 12.5% fetal horse serum, and 500 IU IL-2/ml at 37°C in 5% CO<sub>2</sub>.

### Transfection with small interfering RNA (siRNA)

HEK293E cells were transfected with small interfering RNA (siRNA) specific to TM4SF5 (5'-CCATCTCAGCTTGCAAGTC-3') [18] using Lipofectamine 2000 for 48 h prior to analysis.

### Flow cytometry

To analyze Ab27 and Ab79 binding to TM4SF5, flow cytometry was performed using the SNU449Cp, SNU449Tp, and HEK293E cells that had been transiently transfected with either a TM4SF5-specific siRNA or a negative control siRNA. Cells ( $2 \times 10^5$ ) were incubated with either Ab27 or Ab79 at 0.3 or 1 µg/ml for 45 min at 4°C in PBS containing 1% BSA. The cells were washed twice with 1% BSA/PBS, followed by a 30 min incubation with fluorescein isothiocyanate (FITC)-conjugated anti-human IgG (Fc-specific; Pierce, Rockford, IL, USA). Viable propidium iodide (PI)-negative cells were analyzed for antibody binding using a FACSCalibur (BD Immunocytometry System, San Jose, CA, USA).

### Immunoblot analysis

Whole-cell lysates were prepared using RIPA buffer, immunoblotted as described [19], and analyzed using the following primary antibodies: anti-FAK, anti-phospho-p27 (S10), anti-p27, anti-phospho-FAK (Y577), anti-c-Src, anti-β-actin, and anti-GAPDH (Santa Cruz Biotechnology, Santa Cruz, CA, USA); anti-phospho-FAK (Y925), anti-phospho-c-Src (Y416), anti-phospho-Akt (S473), anti-Akt, anti-phospho-ERK1/2, anti-ERK1/2, and anti-survivin (Cell Signaling, Danvers, MA, USA); anti-phospho-FAK (Y397) (Abcam, Cambridge, UK); anti-TM4SF5 (produced in-house) [8]. A cytosolic fraction was prepared using the Compartmental Protein Extraction Kit (Millipore, Billerica, MA, USA) according to the manufacturer's instructions.

### Immunocytochemistry

SNU449Cp and SNU449Tp cells were plated on coverslips and incubated for 48 h. The cells were then fixed for 20 min in methanol and permeabilized for 1 min with acetone. After blocking in 1% normal horse serum, the cells were incubated with Ab27, Ab79, anti-TM4SF5 (Santa Cruz Biotechnology, sc-165713), or anti-TM4SF5 (Sigma, HPA041259) (5 µg/ml), followed by a corresponding secondary antibody conjugated to FITC or Alexa-546. The cells were

counterstained with 4,6-diamidino-2-phenylindole (DAPI; Sigma) to visualize nuclei. Immunofluorescent images were acquired under a confocal microscope (LSM 510 META; Carl Zeiss, Jena, Germany).

### Co-immunoprecipitation

SNU449 cells were transiently transfected with strep-tagged TM4SF5 [11] (or mock-transfected) for 24 h and then treated with Ab27 or Ab79 (10  $\mu\text{g}/\text{ml}$ ) for an additional 24 h. Cells were lysed in lysis buffer (20 mM HEPES, pH 7.4, 150 mM NaCl, 2 mM  $\text{MgCl}_2$ , 2 mM  $\text{CaCl}_2$ ) containing 1% Brij58. Whole cell lysates (850  $\mu\text{g}/\text{condition}$ ) were immunoprecipitated with streptavidin beads (Thermo Fisher Scientific, Waltham, MA, USA) at 4°C for 16 h. The protein complexes were washed twice with ice-cold lysis buffer and then twice with PBS. The immunoprecipitated proteins were eluted by boiling in SDS sample buffer and analyzed by immunoblotting with anti-Strep tag (IBA; Olivette, MO, USA), anti-integrin  $\alpha 2$  (Chemicon, Temecula, CA, USA), anti-integrin  $\alpha 5$  (BD Biosciences), and anti-CD44 (BioLegend; San Diego, CA, USA) antibodies.

### Internalization analysis

To analyze internalization of cell-surface binding antibody, cells were seeded on coverslips in a six-well plate and incubated at 37°C for 24 h before being incubated with Ab27 or Ab79 (20  $\mu\text{g}/\text{ml}$ ) at 37°C for 30 min or 1, 5, or 12 h. The cells were then fixed in 3.7% paraformaldehyde/PBS at 4°C overnight and permeabilized in 0.3% Triton X-100 for 5 min. After blocking in 2% BSA, the cells were incubated with FITC-conjugated anti-human Fc, washed, and counterstained with DAPI to visualize cell nuclei. Mounted samples were visualized with a confocal microscope (LSM 510 META). Cells were also co-stained with anti-Rab7 (Cell Signaling) and then incubated with tetramethylrhodamine isothiocyanate (TRITC)-conjugated anti-rabbit antibody (Pierce) to determine the endosomal localization of the Ab27 and Ab79 antibodies.

Cell surface binding of Ab27 and Ab79 was also analyzed using flow cytometry. Briefly, cells were incubated with 0.3  $\mu\text{g}/\text{ml}$  Ab27 or Ab79 for 45 min at 4°C, washed to remove unbound antibodies, and then either warmed to 37°C to allow internalization or maintained at 4°C. Cells were transferred to ice-cold buffer to stop the occurrence of internalization and stained with FITC-conjugated anti-human IgG. PI-negative cells were analyzed by flow cytometry. The relative levels of Ab27 or Ab79 bound to the cell surface were calculated as the shift in the fluorescence signal of the antibody occupancy relative to that

detected at the beginning of the internalization period.

### scFv-Fc ELISAs (antigen-binding ELISA)

An EC2-glutathione S-transferase (GST) fusion protein was generated to analyze the binding of the scFv-Fc forms of Ab27 and Ab79 to the TM4SF5 EC2 antigen. A synthetic DNA fragment encoding EC2 followed by GST and a stop codon was subcloned into the *pCMV-Fc-myc* vector. The resulting recombinant EC2-GST fusion protein expression plasmid was transfected into HEK293E cells using Lipofectamine 2000. The culture medium was changed to serum-free medium after 48 h. Conditioned medium was collected at intervals of 2 to 3 days. The EC2-GST fusion protein in conditioned medium was affinity-purified using a Glutathione-Sepharose 4B column (GE Healthcare).

Ninety-six-well Immunoplates (eBiosciences, San Diego, CA, USA) were coated with the purified EC2-GST protein (100 ng/well) diluted in 50 mM sodium carbonate buffer (pH 9.6) at 4°C overnight and then blocked with 2% BSA in PBS. The plates were washed three times with PBS containing 0.05% Tween 20 between all steps. Ab27 or Ab79 (amounts ranging from 0 to 90 ng per well) was added into each well, and then HRP-conjugated anti-human Fc was added. All incubations were carried out at 37°C for 1 to 2 h. Color was developed with TMP substrate solution, and the absorbance was measured at 450 nm using a microplate reader (BMG LABTECH GmbH, Ortenber, Germany).

### Surface plasmon resonance (SPR) analysis

The kinetic parameters of the interaction between the scFv-Fc forms of Ab27 and Ab79 and EC2-GST were determined at 25°C using the Biacore 3000 (GE Healthcare Bio-Sciences AB, Uppsala, Sweden). Briefly, EC2-GST protein was immobilized on a CM5 dextran sensor chip in 10 mM sodium acetate buffer (pH 4.5) using the amine coupling kit and a flow rate of 30  $\mu\text{l}/\text{min}$ . Ab27 or Ab79 in HBS-EP buffer (10 mM HEPES, pH 7.4, 150 mM NaCl, 3 mM EDTA, 0.005% (v/v) surfactant P20) was then injected over 2 min at a flow rate of 30  $\mu\text{l}/\text{min}$ . Data were evaluated using the Biacore BIAevaluation software version 4.1, and the association rate ( $k_a$ ), dissociation rate ( $k_d$ ), and equilibrium dissociation constant ( $K_D$ ,  $k_d/k_a$ ) were calculated to determine binding affinity.

### Invasion and cell migration assays

Invasion and cell migration assays were performed as previously described [19]. For the invasion assays, cells were plated in the presence of antibodies in serum-free medium on Transwell inserts (Corning, NY, USA) coated with 25  $\mu\text{g}$  of Matrigel (BD

Biosciences). The underside of the insert was pre-coated with 2  $\mu\text{g}$  of fibronectin or collagen type I (Sigma). After incubation for 48 h at 37°C in 5%  $\text{CO}_2$ , the inserts were fixed with 3.7% paraformaldehyde/PBS and stained with 2% crystal violet. The numbers of cells that had invaded the Matrigel were counted in five representative ( $\times 100$ ) fields per insert. Cell migration assays were performed in a similar manner but without the Matrigel coating.

### Cell proliferation assay

Cell proliferation was determined using the colorimetric WST-1 Cell Proliferation Assay Kit (Takara Bio Inc., Otsu, Shiga, Japan). Briefly, cells were seeded into 96-well plates at a density of  $5 \times 10^3$  cells/well and incubated for 48 to 72 h in the presence of antibodies. The cells were then incubated with the WST-1 reagent (one-tenth of the medium volume), and formazan dye formation was determined by measuring absorbance at 450 nm using a microplate reader.

### Cell survival analysis and Anoikis assay

Cell survival under suspension culture condition was determined. Briefly, cells at a density of  $5 \times 10^3$  cells/well with antibodies were seeded into 96-well plates with an Ultra-Low Attachment Surface (Corning, NY, USA) and incubated for 7 days in the absence of serum. Cell viability was determined using the colorimetric WST-1 assay as described above.

Cells ( $5 \times 10^5$ ) were seeded in the presence of antibodies into six-well plates with an Ultra-Low Attachment Surface (Corning) to induce anoikis. Cells were washed and stained with 5  $\mu\text{l}$  of annexin V and 5  $\mu\text{l}$  of PI per  $1 \times 10^5$  cells for 15 min at r.t. in the dark, and the percentage of apoptotic cells was analyzed using flow cytometry. The cells were harvested after the induction of anoikis, washed with PBS, and lysed for immunoblot analysis.

### Antibody-dependent cell-mediated cytotoxicity (ADCC) assay

NK-92 cells expressing human CD16 (ATCC) were used as effector cells (E). The expression of CD16 on the NK-92 cells was confirmed using FACSCalibur prior to the assay. The target cells (T) consisted of the SNU449Cp, SNU449Tp, PC3, SW480, HCT-116, HT-29, LS174T, and Colo205 cell lines. These cell lines were seeded into a 96-well plate ( $5 \times 10^3$  of each per well) and incubated with Ab27 for 1 h at 37°C. The cells were then incubated with NK-92 cells at a ratio of E:T 20:1 for 12 h at 37°C. Cytotoxicity was determined using a Cytotoxicity Detection Kit PLUS (LDH) (Roche Applied Science, Mannheim, Germany) to measure the lactate dehydrogenase (LDH) activity

released from the cytosol of damaged cells. Spontaneous (target cells only with antibody), maximum (complete lysis of target cells with the lysis solution provided by the kit), and nonspecific (target cells and effector cells without antibody) releases were also determined. The percentage of specific lysis was calculated according to the manufacturer's instructions as follows: (specific release – nonspecific release) / (maximum release – spontaneous release)  $\times 100$ .

### Mouse xenograft models

All animal procedures were performed in accordance with the procedures of the Seoul National University Laboratory Animal Maintenance Manual and Institutional Review Board (IRB) agreement. Nude mice (BALB/c-nude, 5 weeks old, male) were obtained from Japan SLC, Inc (Japan). SNU449T<sub>7</sub> (stably overexpressing TM4SF5) or SNU449Cp (control) cells were resuspended in PBS and mixed with Matrigel on ice prior to injection. SNU449T<sub>7</sub> or SNU449Cp cells ( $5 \times 10^6$ ) were injected subcutaneously into the back of 18 or 4 mice, respectively. The tumor-bearing mice injected with SNU449T<sub>7</sub> cells were randomized into control and treatment groups ( $n = 6$  per group) after 8 days. Ab27 (5  $\mu\text{g}/\text{mouse}$ ) or Ab79 (16  $\mu\text{g}/\text{mouse}$ ) antibodies were then injected into the tumor in each mouse at 2 or 3 day intervals (total five times). PBS (20  $\mu\text{l}/\text{mouse}$ ) was injected as a negative control. Body weight and tumor volume were measured prior to the antibody injection. The tumor volumes were calculated as follows: tumor volume = ( $\mathbf{a} \times \mathbf{b}^2$ )  $\times 1/2$ , where  $\mathbf{a}$  was the width at the widest point of the tumor and  $\mathbf{b}$  was the maximal width perpendicular to  $\mathbf{a}$ . The mice were sacrificed and photographed 19 days after the injection of the tumor cells. Tumor masses were lysed as previously described [8] and subjected to immunoblot analysis.

### Analysis of The Cancer Genome Atlas (TCGA) data

cBioPortal (www.cbioportal.org) [20, 21] was used to analyze TCGA-generated human colorectal adenocarcinoma data (TCGA, Provisional). All patient samples with available mRNA expression profiles were included in the survival curve analysis.

### Statistical analysis

Statistical analyses were performed using a Student's *t*-test and the Logrank test, where  $P < 0.05$  was considered statistically significant.

## Results

### Selection of TM4SF5 EC2-specific scFv clones

To develop novel monoclonal antibodies binding

to human TM4SF5 EC2, we first purified recombinant human TM4SF5 EC2-Fc fusion protein (EC2-Fc; ~38 kDa) produced in HEK293E cells (Figure 1A). A slight

shift in molecular mass was detected after PNGase F treatment (data not shown), suggesting the presence of glycosylation in the fusion protein.

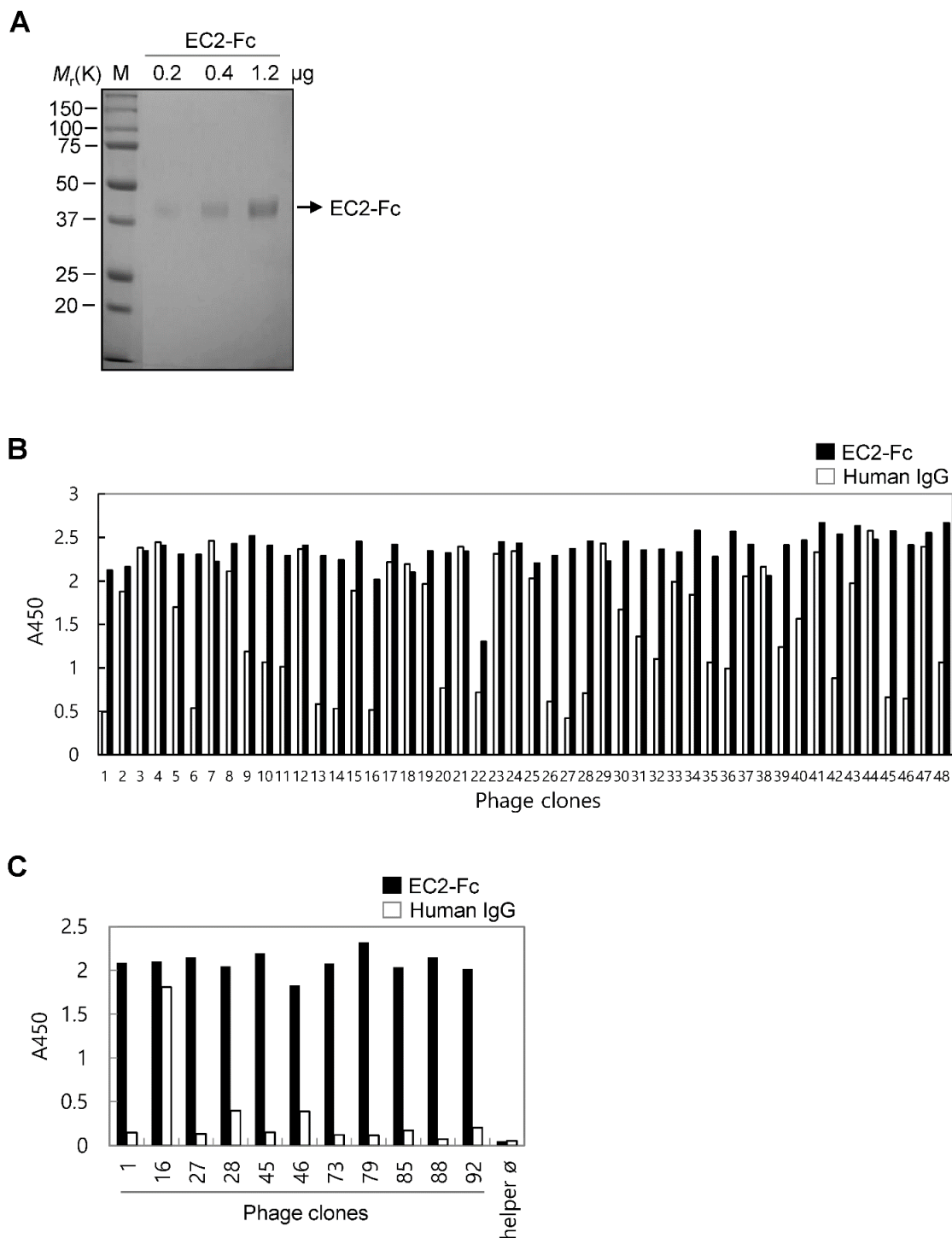


**Figure 1. Selection of TM4SF5 EC2-binding clones from the phage-displayed scFv library. (A)** The recombinant TM4SF5 EC2 fused to the Fc of human immunoglobulin IgG1 protein was produced in HEK293E cells. The secreted protein was purified by protein A affinity chromatography, and analyzed by SDS-PAGE followed by Coomassie brilliant blue staining. M, size marker. **(B)** Screening of individual phage clones using phage ELISA. Ninety-six clones from the second round of panning were tested for binding to TM4SF5 (data for 48 clones are shown). Human IgG was used as negative control to exclude Fc-binding clones. **(C)** Specific binding of ten clones to the TM4SF5 EC2. Clone#16 was an Fc-binding clone.

The purified EC2-Fc fusion protein was used in panning studies to select TM4SF5-specific antibodies. Pre-clearing the library phages by subtraction panning against human IgG depleted the Fc-specific binding phages. The pre-cleared phages were then used for panning against the EC2-Fc protein. The enriched pool resulting after the second round of panning was used for the subsequent screening of TM4SF5-specific individual clones (Figure 1B). Twenty of the ninety-six clones tested were positive for TM4SF5-specific binding recognizing the EC2-Fc fusion protein but not human IgG. DNA sequence analysis revealed ten unique clones binding to the EC2-Fc protein (Figure 1C). Using preliminary flow cytometry analysis (data not shown), two clones, Ab27 and Ab79, possessing homologous amino acid sequences of the complementary determining regions were selected for further characterization.

We constructed Ab27 and Ab79 as scFv-Fc (scFv fused with Fc) chimeric antibodies. The Fc domain was derived from human IgG1 because human IgG1 is the most effective human IgG subclass to mediate

antibody-dependent cell-mediated cytotoxicity (ADCC) and complement-dependent cytotoxicity (CDC) effector functions [22]. All of the assays in this study were performed using Ab27 and Ab79 scFv-Fc chimeric antibodies (~50 kDa; Supplementary Figure S1A). To determine the binding affinity of Ab27 and Ab79 for TM4SF5 EC2, EC2-GST fusion protein was produced, purified by affinity chromatography (Supplementary Figure S1B), and used as an antigen. Antigen-binding ELISA showed that, while both Ab27 and Ab79 bound significantly to EC2-GST, Ab27 bound more strongly than Ab79 (Figure 2A). The kinetics of the interaction of Ab27 and Ab79 with EC2-GST were examined by surface plasmon resonance (SPR) analysis. The binding affinity ( $K_D$ ) of Ab27 and Ab79 was approximately 9.2 nM and 16.9 nM, respectively (Figure 2B). These results show that the Ab27 (more strongly) and Ab79, chimeric antibodies to TM4SF5 generated in this study bound specifically and strongly with the human TM4SF5 EC2 protein.

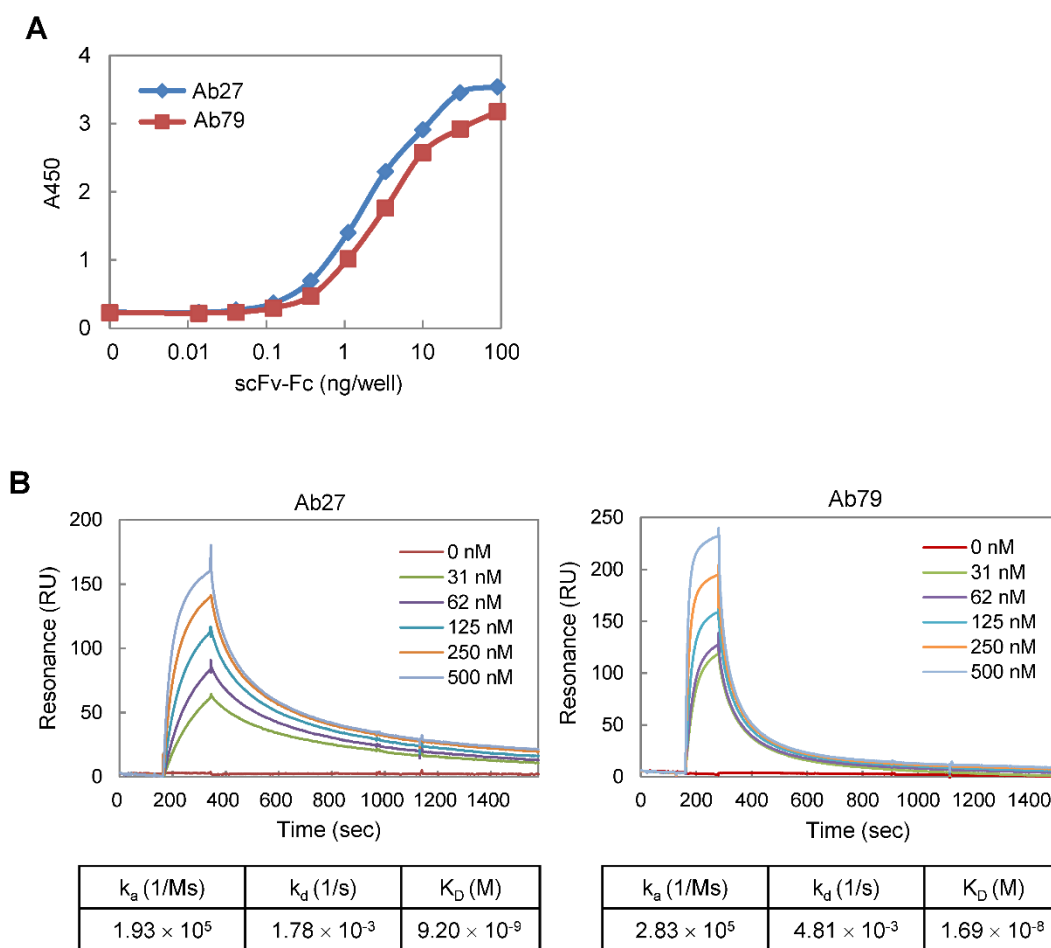
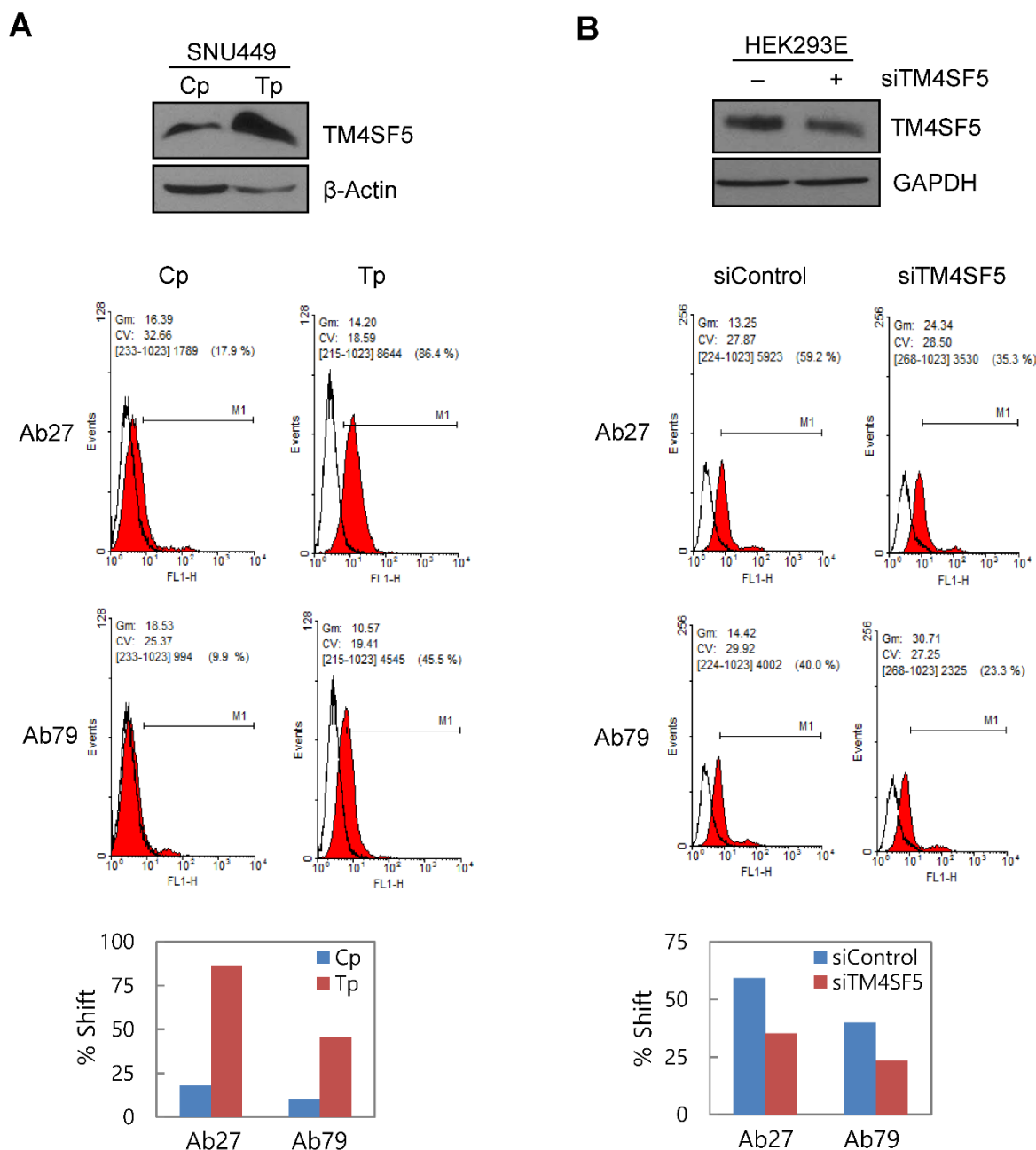


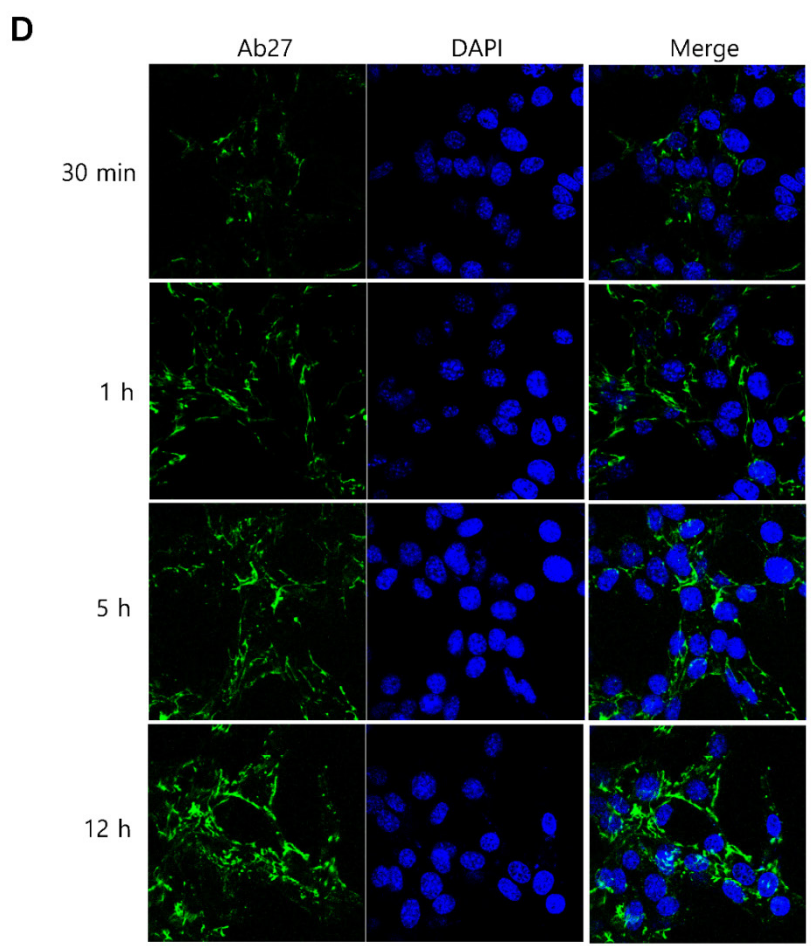
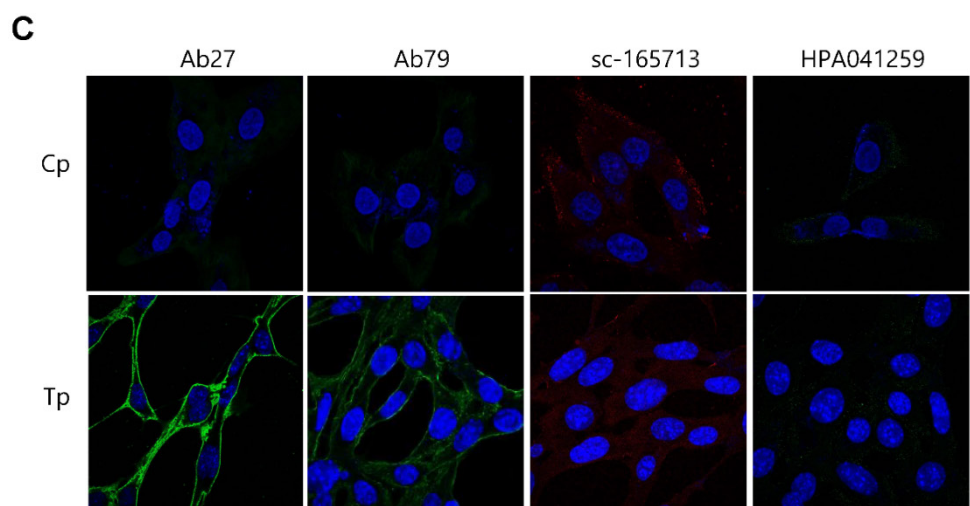
**Figure 2. Affinity determination of anti-TM4SF5 monoclonal antibodies.** (A) Antigen-binding activities of Ab27 and Ab79 were determined by antigen-binding ELISA. Immunoplate wells were coated with the recombinant human TM4SF5 EC2-GST (EC2-GST) fusion protein (100 ng/well), and then incubated with varying amounts of Ab27 or Ab79. Bound antibodies were detected by HRP-conjugated anti-human Fc. (B) Ab27 and Ab79 antigen-binding affinities were analyzed using Biacore. The recombinant EC2-GST fusion proteins were immobilized on a sensor chip, and increasing amounts of Ab27 or Ab79 were applied. Kinetic parameters of binding reaction are shown under the sensorgrams.

### Binding of Ab27 and Ab79 to TM4SF5 expressed on the cell surface

To determine whether Ab27 and Ab79 recognize TM4SF5 on the cell surface, we performed flow cytometric analyses with SNU449Cp (vector-transfectant), SNU449Tp (TM4SF5-overexpressing transfectant), and HEK293E cells transiently transfected with TM4SF5-specific siRNA or negative control siRNA. Both Ab27 and Ab79 bound to the SNU449Tp cells more efficiently than to the SNU449Cp cells. This result correlated with the relative expression level of TM4SF5 present in the SNU449Cp cells versus the SNU449Tp cells

determined by immunoblot analysis (Figure 3A). Similarly, suppression of TM4SF5 expression by siRNA in HEK293E cells resulted in reduced binding to the cells by both antibodies (Figure 3B). Ab27 bound more strongly than Ab79, which is consistent with the affinity shown in Figure 2. In addition, immunofluorescence staining showed that Ab27 (more strongly) and Ab79 stained the membrane edges of SNU449Tp cells but not those of control SNU449Cp cells (Figure 3C). However, two commercial anti-TM4SF5 antibodies tested in parallel did not appear to substantially or specifically bind TM4SF5 (Figure 3C).





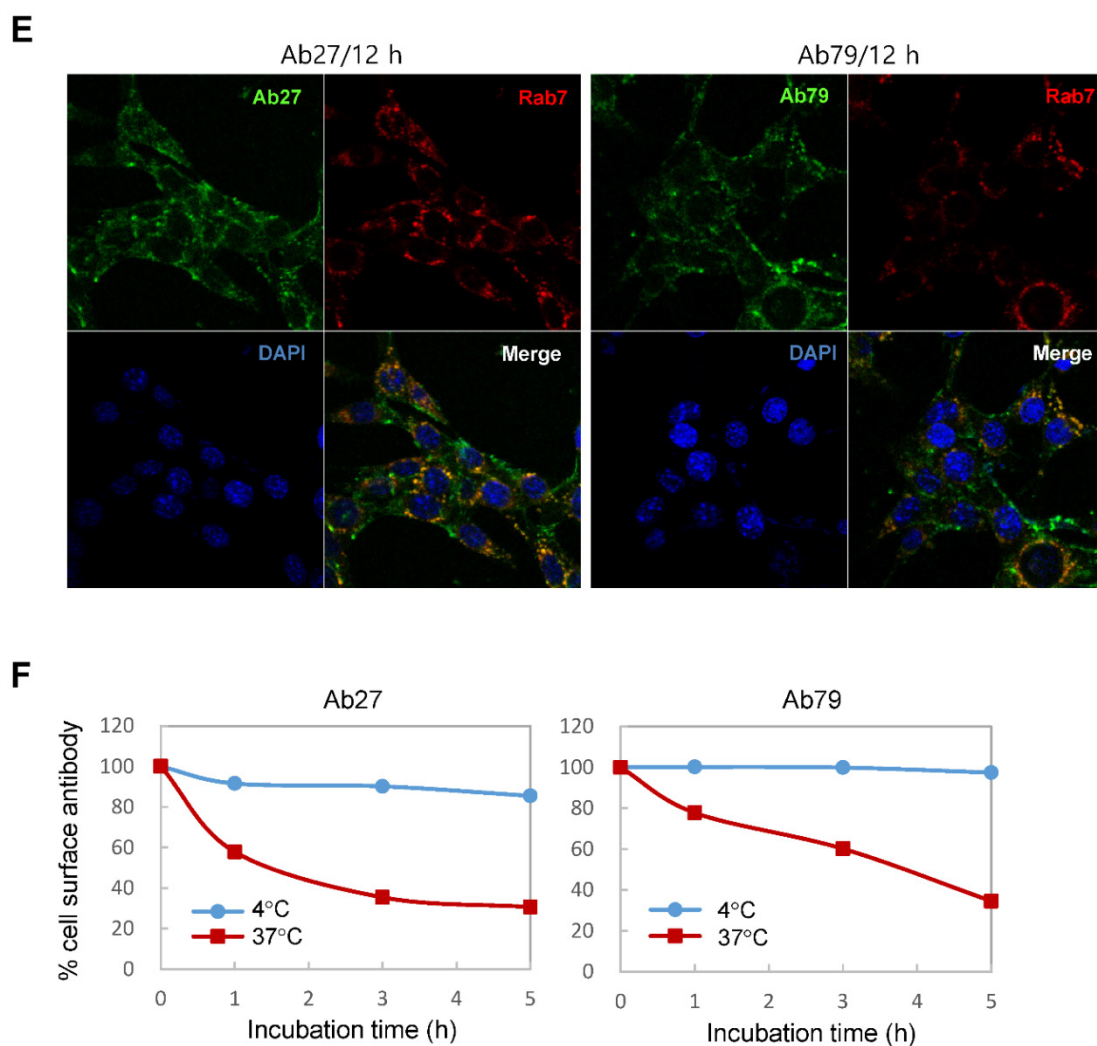


**Figure 3. Binding and internalization of Ab27 and Ab79 to TM4SF5 expressed on the cell surface.** (A) Upper: immunoblot analysis of TM4SF5 using lysates from SNU449Cp and SNU449Tp cells. TM4SF5 was detected by rabbit anti-TM4SF5 (in-house) [8].  $\beta$ -Actin was used as an internal control. Lower: flow cytometry analysis of SNU449Cp and SNU449Tp cells labeled with Ab27 and Ab79. The colored populations indicate TM4SF5 staining while the uncolored populations show control staining. The extent of a shift in the fluorescence signal compared to control staining, which represented the binding activity of antibody, is shown as a graph. (B) HEK293E cells were transfected with TM4SF5-specific siRNA or control siRNA for 48 h prior to analysis. Immunoblot and flow cytometry analyses were performed as in (A). (C) SNU449Cp and SNU449Tp cells were immunostained with Ab27, Ab79, and two commercial anti-TM4SF5 antibodies (sc-165713 and HPA041259), followed by a corresponding secondary antibody conjugated to FITC (Ab27, Ab79, and HPA041259) or Alexa-546 (sc-165713). Cell nuclei were stained with DAPI. Merged images are shown. (D) Confocal microscopic analysis of Ab27 internalization. SNU449Tp cells were incubated with Ab27 (20  $\mu$ g/ml) at 37°C for the indicated time periods. Ab27 was detected using FITC-conjugated anti-human Fc (green), and the nuclei were counterstained with DAPI (blue). (E) SNU449Tp cells were incubated with Ab27 or Ab79 (20  $\mu$ g/ml) at 37°C for 12 h and were stained using FITC-conjugated anti-human Fc (green) and anti-Rab7 followed by TRITC-conjugated anti-rabbit antibody (red). Cells were counterstained with DAPI. (F) SNU449Tp cells were incubated with Ab27 (0.3  $\mu$ g/ml) for 45 min at 4°C, washed to remove unbound antibodies, and either warmed to 37°C to allow internalization or maintained at 4°C for the indicated time periods. Cells were stained with FITC-conjugated anti-human Fc and analyzed by flow cytometry.

### Internalization of Ab27 and Ab79 into cancer cells

To examine whether Ab27 is internalized after binding to the cells, we incubated TM4SF5-overexpressing SNU449Tp cells with Ab27 for the indicated time periods at 37°C before the cells were fixed, permeabilized, and immunostained. Ab27 bound to the plasma membrane of the cells after 1 h, and substantial amounts of the antibody were internalized into endocytic vesicles of the cells from 5 to 12 h after the antibody treatment (Figure 3D). Double immunostaining showed that the internalized antibody was colocalized with Rab7, a late endosome

marker at 12 h after the antibody treatment (Figure 3E), indicating that Ab27 caused the translocation of TM4SF5 from the cell surface into the endosome. Ab79 was also internalized from the cell surface and colocalized with the late endosome after 12 h (Figure 3E). On the other hand, only a small amount of cell surface binding or internalization of the antibodies was detected in the SNU449Cp cells (data not shown), a result that was probably due to the presence of lower levels of TM4SF5 in these cells than in the SNU449Tp cells.

The SNU449Tp cells were incubated with Ab27 and Ab79 for 45 min at 4°C and then either warmed to 37°C to allow internalization or maintained at 4°C.

The residual levels of cell surface Ab27 and Ab79 were analyzed by flow cytometry to determine whether Ab27 and Ab79 downregulated TM4SF5 from the cell surface. The levels of cell surface-bound Ab27 and Ab79 were substantially reduced following incubation at 37°C but not at 4°C (Figure 3F), suggesting that Ab27 and Ab79 caused reduction of the cell surface TM4SF5 level. These observations indicate that Ab27 and Ab79 are internalized into target cancer cells after binding to TM4SF5 where they then downregulate TM4SF5 from the cell surface.

### Effects of Ab27 and Ab79 on cancer cell proliferation, invasion, and survival

We previously reported that TM4SF5 was upregulated in HCC [8]. In the current study, analysis of TCGA-generated colorectal adenocarcinoma data (TCGA, provisional) showed that patients whose colorectal tumors expressed high levels of TM4SF5 ( $Z > 1.5$ ) had a significantly worse overall survival than those patients with lower levels of TM4SF5 ( $Z \leq 1.5$ ) in their tumors ( $n = 382$ ,  $P = 0.0391$ ) (Supplementary Figure S2). These results suggest a potential role for TM4SF5 in cancer development and/or progression in the colon as well as liver.

TM4SF5 influences/activates intracellular signaling pathways mediating cell proliferation, migration, and invasion for tumor progression and maintenance [8]. We therefore evaluated the effects of Ab27 and Ab79 on cell proliferation and invasion using cancer cells expressing either endogenous TM4SF5 or stably overexpressing TM4SF5. Immunoblot analysis showed that TM4SF5 was detected in all of the cell lines tested, although the levels of TM4SF5 were dependent upon the cell lines (Figure 4A). Ab27 and Ab79 significantly reduced the proliferation of HCT-116, HT-29, and LS174T colon cancer cells over a 3-day period (Figure 4B). Ab27 and Ab79 also moderately reduced the proliferation of SNU449T<sub>7</sub> and SNU449T<sub>p</sub> cells for 48 h (Figure 4C). However, the commercial anti-TM4SF5 antibody (sc-165713) did not reduce the proliferation of TM4SF5-expressing cancer cells (Supplementary Figure S3). Ab27 and Ab79 did not, however, significantly affect the proliferation of the SW480 and PC3 cell lines that display low levels of endogenous TM4SF5 (data not shown). The influence of Ab27 and Ab79 on cell migration and cell invasion through a reconstituted basement membrane (Matrigel) was examined. Ab27 substantially reduced the invasion and migration of HCT-116 and Colo205 colon cancer cells (Figure 4D). Ab79 also reduced the invasion and migration of HCT-116 cells (Supplementary Figure S4A).

We then examined for changes in

TM4SF5-dependent intracellular signaling in LS174T, HCT-116, and HT-29 cells treated with Ab27 and Ab79 for 72 h. TM4SF5 was previously shown to activate FAK and c-Src and cause the induction and phosphorylation of p27<sup>Kip1</sup> enabling its cytosolic translocation for its role in facilitating EMT and cell migration [8]. As shown in Figure 4E, Ab27 and Ab79 reduced the phosphorylation of FAK (HT-29, moderately; LS174T, strongly) and c-Src (HCT-116, moderately; LS174T, strongly) and the expression of p27<sup>Kip1</sup>. Of note, treatment with recombinant Fc protein had a moderate effect on FAK phosphorylation in HT-29 and LS174T cells and on p27<sup>Kip1</sup> expression in HT-29 cells. The effects of Ab27 and Ab79 were compared with those of recombinant Fc protein (Neg. Fc).

To examine the effect of Ab27 and Ab79 on the interaction between TM4SF5 and integrin  $\alpha 2$ , integrin  $\alpha 5$ , or CD44, we performed co-immunoprecipitation studies using lysates from mock-transfected SNU449 cells or SNU449 cells overexpressing strep-tagged TM4SF5. Consistent with previous results [10, 11, 13], we found that integrin  $\alpha 2$ , integrin  $\alpha 5$ , and CD44 co-precipitated with strep-tagged TM4SF5. The interaction between TM4SF5 and integrin  $\alpha 2$ , integrin  $\alpha 5$ , or CD44 was substantially disrupted by Ab27 and Ab79 (Figure 4F).

Furthermore, we examined whether Ab27 and Ab79 could influence the survival of TM4SF5-expressing cancer cells under suspension culture conditions. HCT-116 cells were incubated in the presence of antibody in low-attachment plates for 7 days. Ab27 and Ab79 significantly reduced cell survival in suspension (Figure 4G). The induction of anoikis sensitivity was also examined by using flow cytometric analysis to determine the percentages of apoptotic cells. Treatment of cells in suspension with Ab27 and Ab79 resulted in a moderate increase in anoikis of HCT-116 cells (Figure 4H), which was accompanied by a reduction of survivin (Figure 4I).

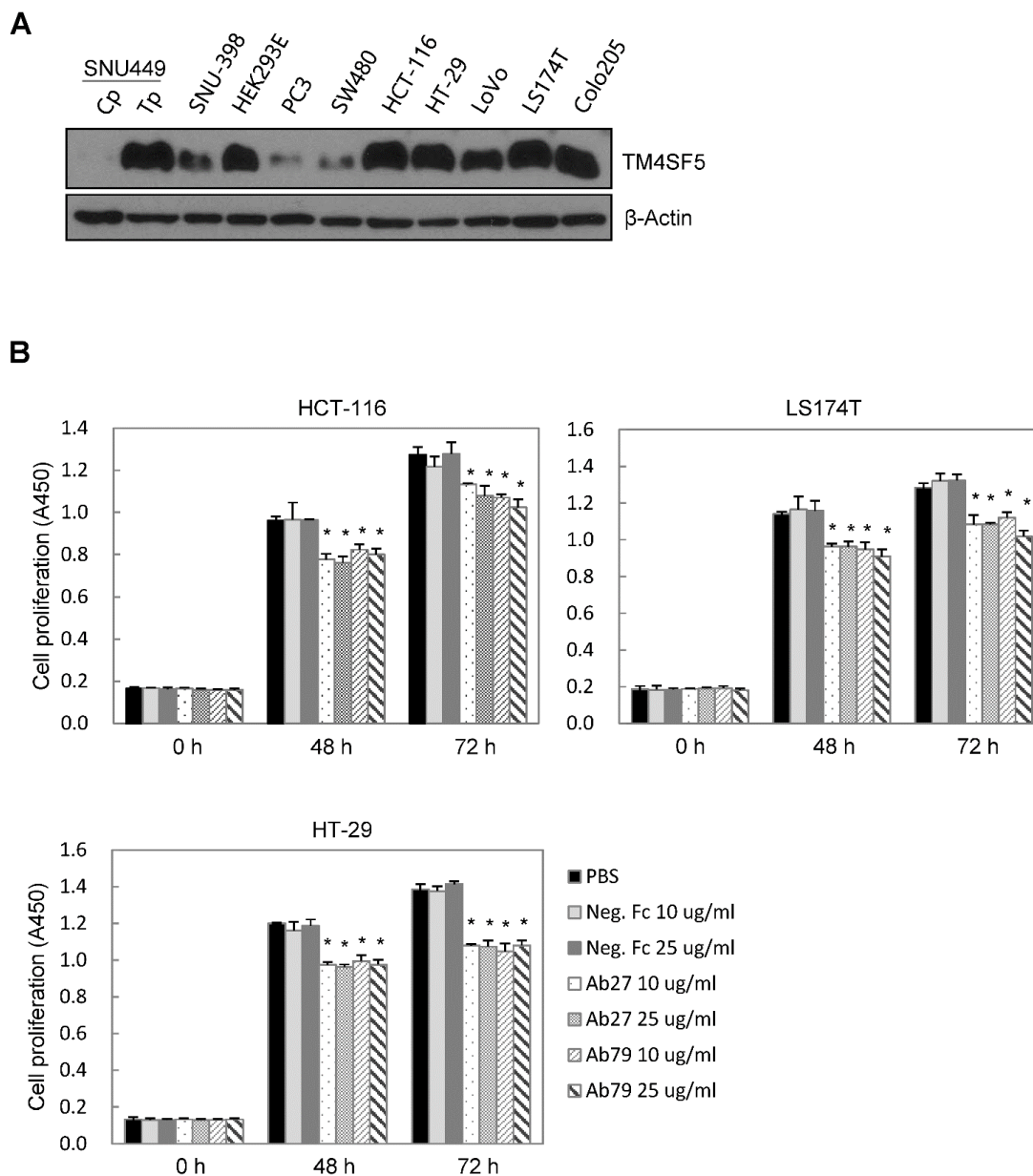
These results indicate that Ab27 and Ab79 suppress TM4SF5-mediated intracellular signaling and inhibit the proliferation, invasion, and survival of TM4SF5-expressing cancer cells.

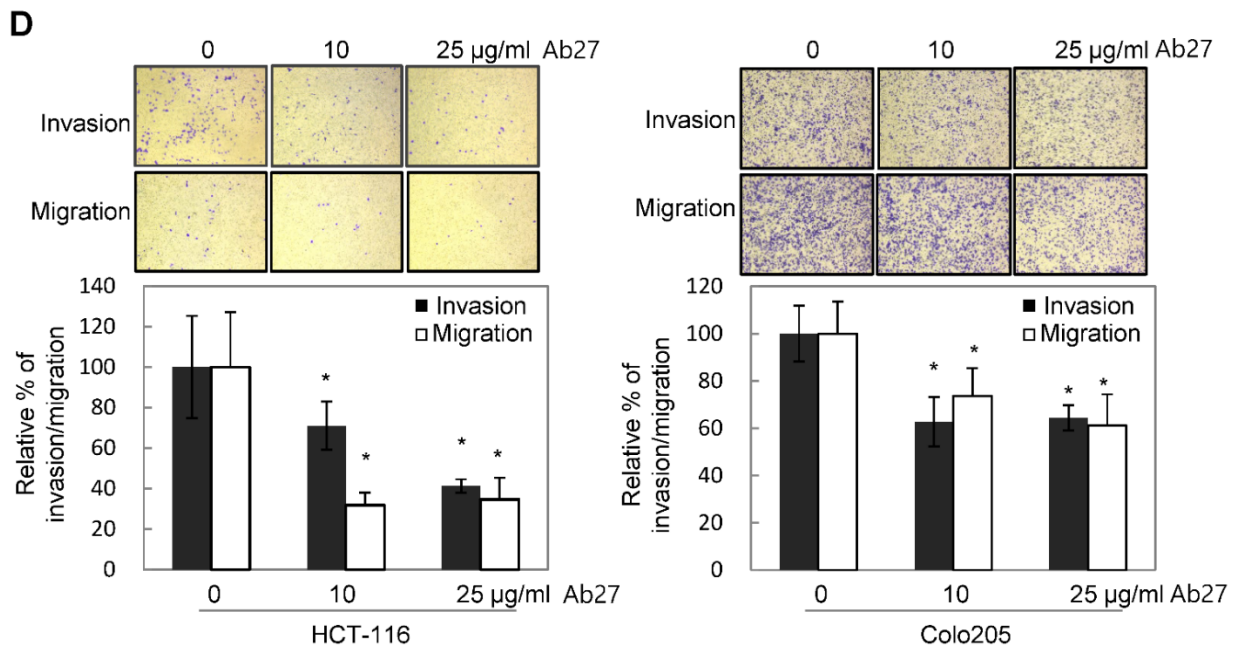
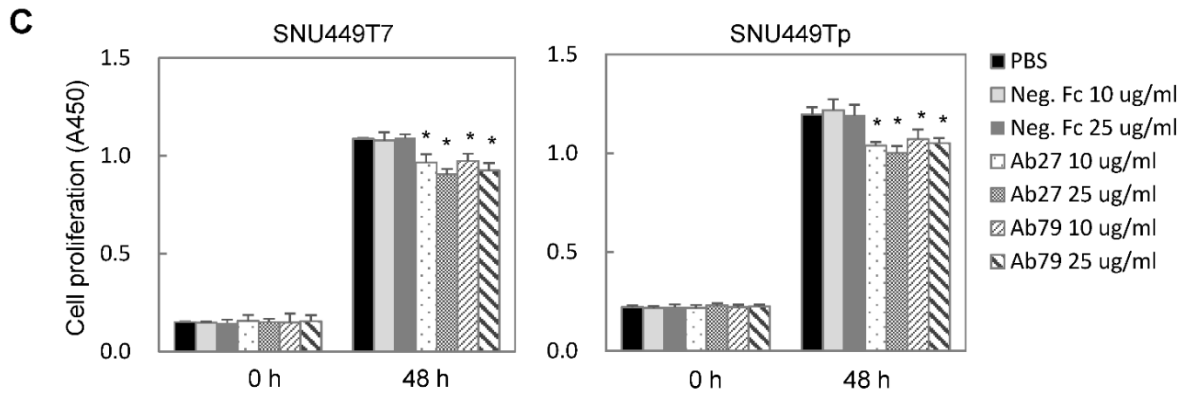
### Ab27-mediated ADCC against TM4SF5-expressing cancer cells

ADCC requires the presence of target-specific antibody and cytotoxic immune cells, such as NK cells and macrophages, which express an Fc receptor. It is an important mechanism involved in the antitumor activity of therapeutic antibodies such as trastuzumab [23]. We therefore examined whether Ab27 could mediate ADCC against TM4SF5-positive cancer cells in a co-incubation assay with CD16-expressing NK-92

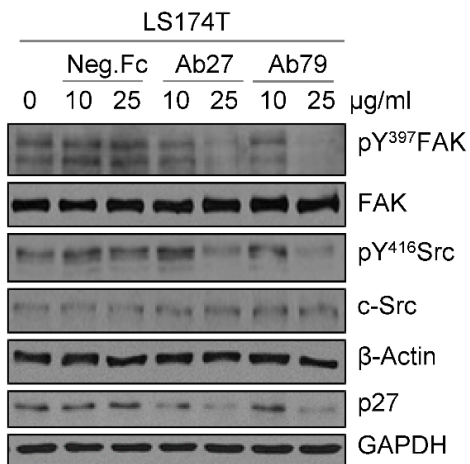
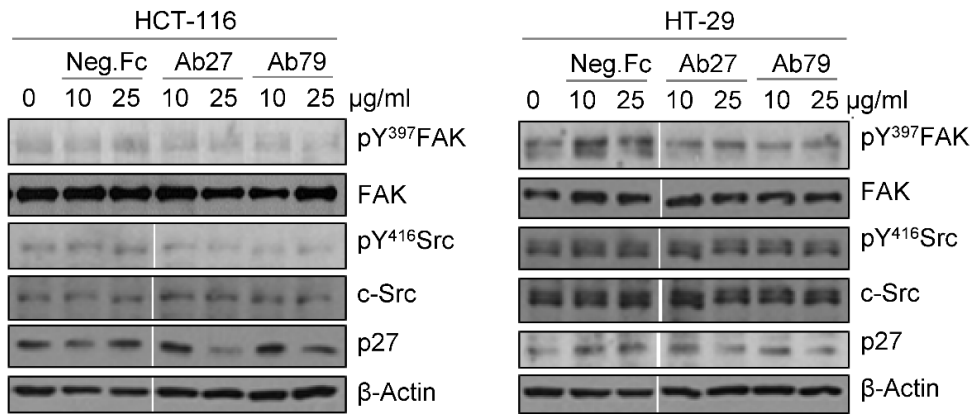
cells. The presence of the Fcγ receptor III (CD16) that is required for ADCC on the NK cell line was confirmed by flow cytometry analysis (Supplementary Figure S4B). Cytotoxicity was measured using a standard lactate dehydrogenase (LDH) assay. The addition of Ab27 resulted in the lysis of approximately 10–15% of the SNU449Tp, HCT-116, HT-29, LS174T, and Colo205 cells, which

express high levels of TM4SF5. A low level of specific lysis was observed in the SNU449Cp, PC3, and SW480 cells, which express relatively low levels of TM4SF5 (Figure 5A and B). Ab27 effectively induced ADCC against HT29 cells in a dose-dependent manner (Figure 5C). Ab79 also exhibited modest ADCC activity (data not shown).

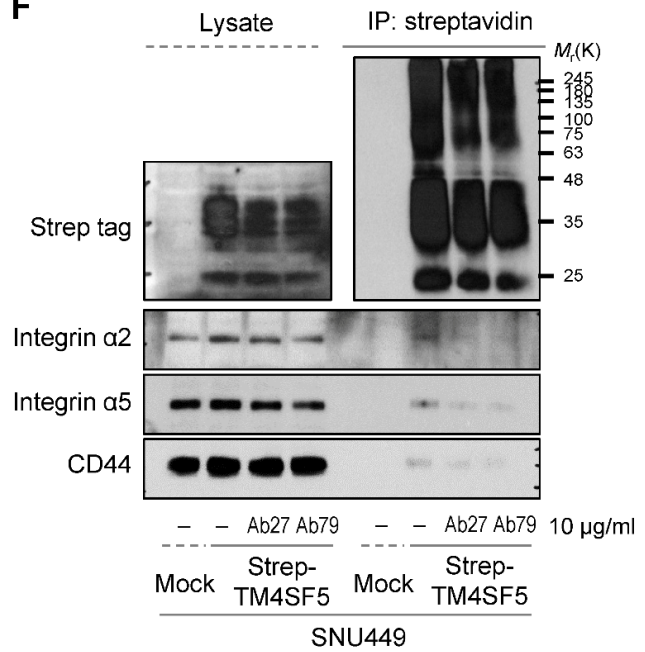




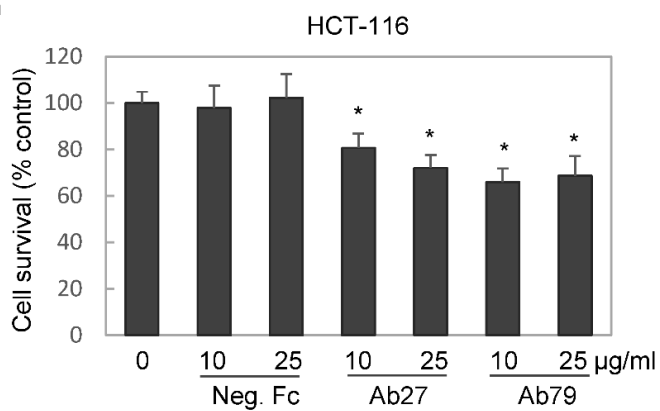
**E**



**F**



**G**



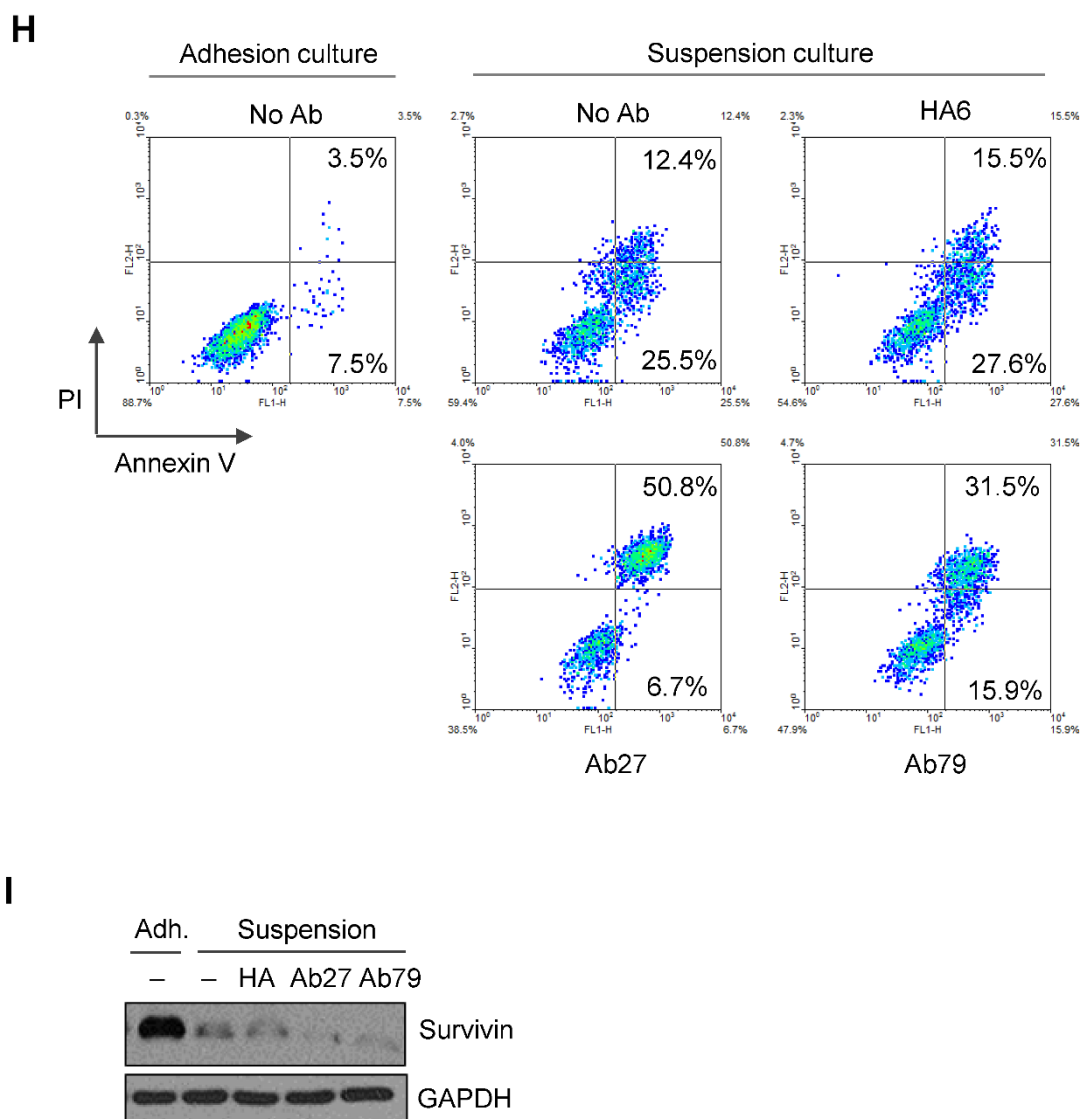


**Figure 4. Ab27 and Ab79 significantly inhibited proliferation, invasion, and survival of cancer cells. (A)** Immunoblot analysis of TM4SF5 in cells. TM4SF5 was detected by a rabbit anti-TM4SF5 (in-house) [8].  $\beta$ -Actin was used as an internal control. **(B)** Colon cancer cells were seeded into 96-well plates at a density of  $5 \times 10^3$  cells/well in the presence of antibodies and incubated for up to 72 h. Cell proliferation was determined by the colorimetric WST-1 assay. **(C)** SNU449T<sub>7</sub> and SNU449T<sub>p</sub> cells were seeded into 96-well plates at a density of  $5 \times 10^3$  cells/well in the presence of antibodies and incubated for 48 h to determine cell proliferation. **(D)** Cells were allowed to invade Matrigel ( $2 \times 10^4$  cells for HCT-116 and  $1 \times 10^5$  cells for Colo205) or migrate ( $1 \times 10^4$  cells for HCT-116 and  $1 \times 10^5$  cells for Colo205) in the presence of antibody for 48 h. The number of cells that had invaded or migrated was counted in five representative ( $\times 100$ ) fields per Transwell insert. Values represent mean  $\pm$  standard deviation (SD). \*  $P < 0.05$ . **(E)** Cells were incubated with antibodies for 72 h prior to lysis. Whole-cell lysates were analyzed by immunoblotting. The cytoplasmic fraction was prepared from the LS174T cells to detect p27.  $\beta$ -Actin or GAPDH was used as an internal control. **(F)** Co-immunoprecipitation was performed to examine the effect of Ab27 and Ab79 on the interaction between TM4SF5 and integrin  $\alpha 2$ , integrin  $\alpha 5$ , or CD44, as described in the Materials and Methods. An anti-strep tag antibody was used to detect strep-tagged TM4SF5. **(G)** To induce anoikis, HCT-116 cells were seeded into 96-well plates with an Ultra-Low Attachment Surface at a density of  $5 \times 10^3$  cells/well in the presence of antibodies and incubated for 7 days. Cell viability was determined by the colorimetric WST-1 assay. Values represent mean  $\pm$  standard deviation (SD). \*  $P < 0.05$ . **(H)** HCT-116 cells were incubated with antibodies (25  $\mu$ g/ml) for 12 h under suspension culture conditions and then stained with annexin V and PI for flow cytometry analysis. **(I)** HCT-116 cells were incubated with antibodies (25  $\mu$ g/ml) for 24 h under suspension culture conditions prior to lysis for immunoblot analysis. GAPDH was used as a loading control. Recombinant Fc protein (Neg. Fc; B, C, E, and G) or HA6 (H and I) was used as a negative control.

### Inhibition of tumor growth in nude mice by Ab27 and Ab79

We next investigated the antitumor efficacy of Ab27 and Ab79 in nude mice bearing TM4SF5-overexpressing SNU449T<sub>7</sub> xenografts. As shown in Figure 6A and B, an intratumoral injection of Ab27 (5  $\mu$ g/mouse/time) and Ab79 (16  $\mu$ g/mouse/time) at 2 or 3 day intervals (total five times) significantly inhibited tumor growth by 66%

without affecting body weight. Immunoblot analysis of xenograft tumor tissues showed that Ab27 and Ab79 reduced phosphorylation of FAK, c-Src, and p27<sup>Kip1</sup> but did not change the phosphorylation of ERK1/2, as expected (Figure 6C), based on the previous observation that TM4SF5 did not affect ERK1/2 activation [8]. Akt phosphorylation was not substantially changed by treatment with Ab27 and Ab79 (Figure 6C), suggesting that other intracellular signaling activities were involved in phosphorylation

of p27<sup>Kip1</sup> *in vivo*, for example, JNK [24], leading to cytosolic p27<sup>Kip1</sup> playing a pro-migratory role. Taken together, these results suggest that Ab27 and Ab79 can inhibit tumor growth in nude mice bearing liver cancer xenografts.

## Discussion

In this study, we generated novel anti-TM4SF5 monoclonal antibodies that bound to the EC2 domain of TM4SF5 by screening a phage-displayed mouse scFv library. The function and efficacy of the resulting Ab27 and Ab79 chimeric antibodies containing human Fc (scFv-Fc) were evaluated to assess the potential of these antibodies as innovative therapeutic agents against liver and colon cancers. Our results demonstrate that Ab27 efficiently recognized TM4SF5 on the cell surface, inhibited the migration, invasion, and proliferation of cancer cells, and reduced tumor growth in nude mice bearing a HCC xenograft. In addition, binding of Ab27 to TM4SF5-positive cancer cells led to the internalization of TM4SF5, resulting in the downregulation of cell surface TM4SF5 and enhancing anoikis sensitivity probably through a reduction in the level of survivin. The addition of

Ab27 was also able to reduce FAK/c-Src activation and p27<sup>Kip1</sup> expression as well as mediating ADCC in TM4SF5-positive tumor cell lines. These results support the potential of Ab27 as an agent for the treatment of TM4SF5-expressing cancers.

The antitumor activity of Ab27 and Ab79 *in vivo* can be explained, at least in part, by the direct tumor-suppressing activity demonstrated by these chimeric antibodies *in vitro*. The ADCC activity of those antibodies may have also contributed to the suppression of tumor growth found *in vivo*. ADCC is an important mechanism underlying the antitumor efficacy of therapeutic antibodies such as trastuzumab. This humanized monoclonal antibody against HER2 is approved for the treatment of HER2-overexpressing breast and gastric cancers. Although several mechanisms, including ADCC and the inhibition of HER2-mediated signaling, were proposed to account for the antitumor activity of trastuzumab, the mechanisms of antitumor activity of trastuzumab are still incompletely defined [23]. Our results show, for the first time, that a monoclonal antibody against TM4SF5 was able to induce ADCC and thus holds promise as a therapeutic antibody.

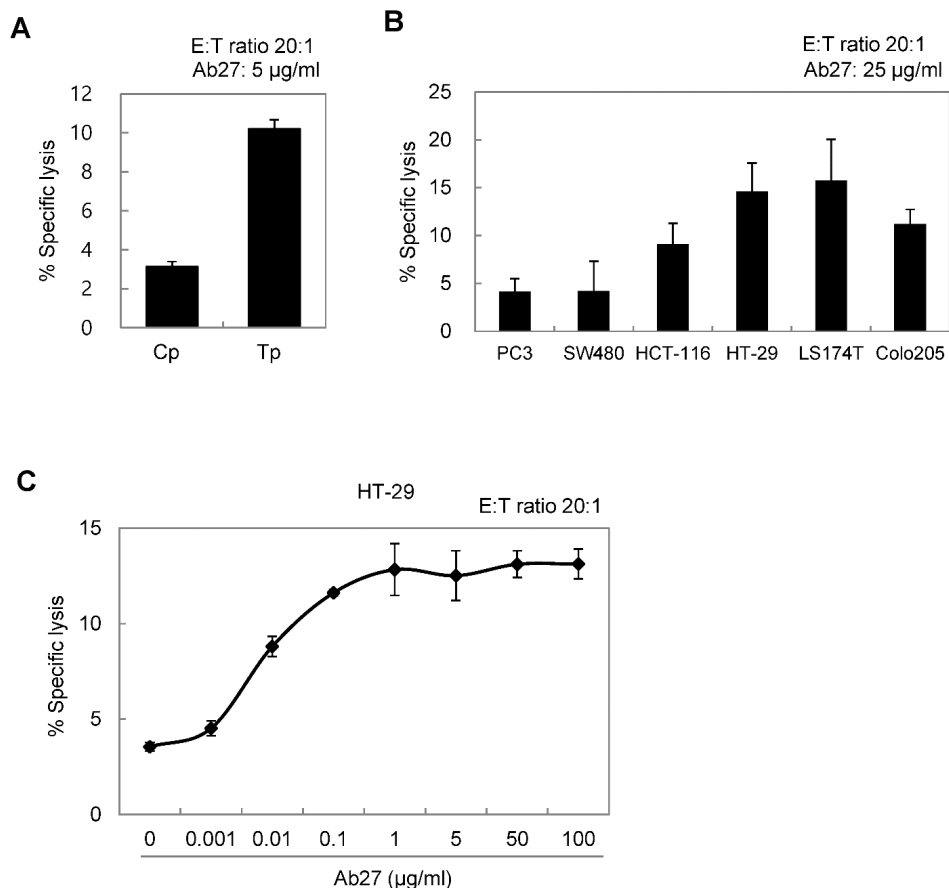


**Figure 5. Ab27 induced ADCC against TM4SF5-expressing cancer cells. (A)** ADCC assay using SNU449Cp and SNU449Tp (target cells, T) and CD16-expressing NK-92 cells (effector cells, E). The ratio of E:T was 20:1. **(B)** ADCC assay against cancer cells expressing endogenous TM4SF5 (target cells) as in (A). **(C)** ADCC assay against HT-29 cells using Ab27 in a dose-dependent manner. Values represent mean  $\pm$  standard deviation (SD). \*  $P < 0.05$ .

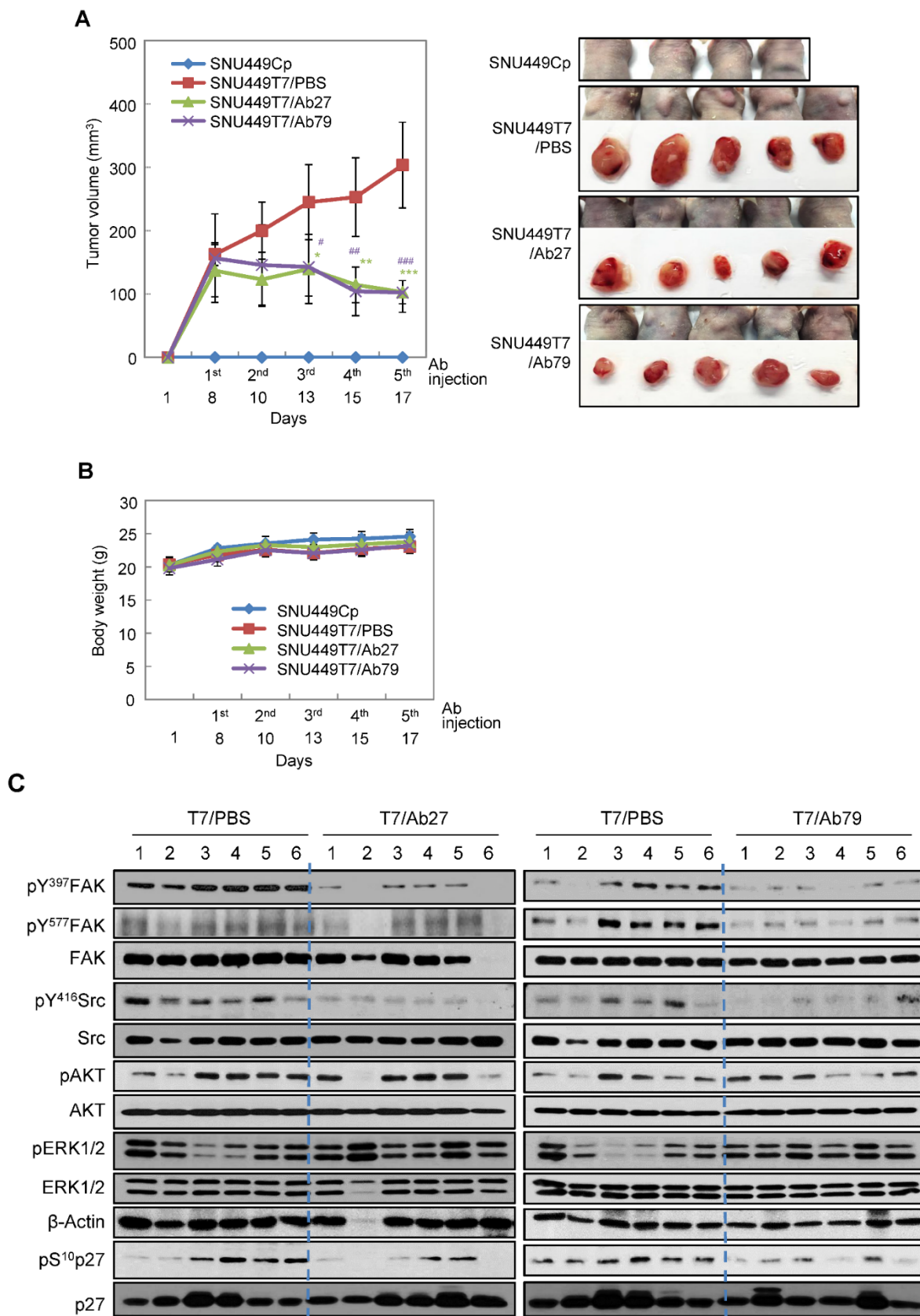


**Figure 6. Therapeutic efficacy of Ab27 and Ab79 against HCC tumor growth in a xenograft mouse model.** SNU449Cp (n = 4) and SNU449T<sub>7</sub> (n = 18) cells were injected subcutaneously into nude mice. On day 8, tumor-bearing mice injected with SNU449T<sub>7</sub> cells were randomized into control and treatment groups (n = 6 each). Ab27 (5 μg/mouse) or Ab79 (16 μg/mouse) were injected into the tumor in each mouse at intervals of 2 to 3 days (total five times). **(A)** Left: Tumor volume (length × width<sup>2</sup> / 2). Value of the minimum per group was excluded for the mean calculation. Values represent mean ± standard deviation (SD). \*P = 0.0138, \*\*P = 0.0115, \*\*\*P = 0.0028, #P = 0.0284, ###P = 0.0017, ####P = 0.0006. Right: Photos of tumor-bearing mice and dissected tumor masses on day 19. Tumors were not detected following the injection of the SNU449Cp cells. **(B)** Body weights of injected mice. Values represent mean ± standard deviation (SD). **(C)** Immunoblot analysis of tumor extracts. β-Actin was used as an internal control.

We previously observed that Ab27 could detect TM4SF5 in human liver cancer tissues and in TGF- $\beta$ -activated hepatocytes [11, 25], confirming that TM4SF5 is overexpressed in human HCC. Furthermore, TM4SF5 plays a critical role in liver fibrosis [25, 26], which can then progress to cirrhosis and subsequently to HCC. We also observed that Ab27 and Ab79 suppressed the fibrotic phenotype in a CCl<sub>4</sub>-mediated mouse liver fibrosis model (unpublished results), evidence supporting the potential of those antibodies as anti-fibrosis therapeutic agents to prevent the progression to HCC. Considering that both Ab27 and Ab79 inhibited invasion and cell migration more efficiently than proliferation, the evaluation of the metastasis-suppressing activity of those antibodies *in vivo* is warranted.

The internalization experiments indicated that Ab27 was internalized into endocytic vesicles, suggesting that TM4SF5 bound by Ab27 may translocate into the endosome and then further into the lysosome. In addition, the level of cell surface-bound Ab27 was decreased after binding to TM4SF5, indicating that Ab27 caused the downregulation of TM4SF5 from the cell surface, a step that might lead to a reduction in the function of TM4SF5. In keeping with this possibility, the 225 monoclonal antibody targeting the EGFR (murine parent antibody of cetuximab) was reported to be rapidly internalized into target tumor cells within 1 h [27] and result in the partial downregulation of EGFR [28].

At present, sorafenib, a multi-kinase inhibitor that inhibits Raf-1, B-Raf, vascular endothelial growth factor receptors, and platelet growth factor receptor, is the only systemic therapy that has demonstrated an overall survival benefit in patients with advanced HCC [2]. The survival benefit was, however, modest in the advanced stages of the disease, and new agents with superior efficacy and/or agents affecting other cellular pathways are needed for treatment of advanced HCC [2]. The use of EGFR-targeting antibodies (cetuximab or panitumumab) in combination with chemotherapy is approved for metastatic colorectal cancer patients with KRAS wild-type [29]. Patients with KRAS mutations are resistant to the anti-EGFR antibodies, and only up to a third of the KRAS wild-type subpopulation respond to EGFR inhibition [29]. Thus, there also remains an urgent unmet need for the identification of potential molecular targets/pathways and the development of novel effective therapeutics for metastatic colorectal cancer.

TM4SF5 is aberrantly expressed in liver, colon, pancreatic, and esophageal cancers [7-9], and plays

important roles in tumor development and progression by enhancing cell proliferation, migration, and invasion [8]. A high level of TM4SF5 is associated with poor survival of esophageal [9] and colorectal (Supplementary Figure S2) cancer patients. We also found that high TM4SF5 expression in lung adenocarcinoma patients was significantly correlated with decreased overall survival ( $n = 1926$ ,  $P = 0.0026$ ) when survival within previously published data sets was analyzed using the kmPlotter (data not shown). In addition, TM4SF5-mediated EMT may have an important function in the resistance of lung cancer cells to EGFR kinase inhibitors (e.g., gefitinib) [12]. Blockade of TM4SF5 by the TM4SF5-targeting agent, TSAHC, suppressed tumor growth [14] and liver fibrosis [26]. TSAHC also inhibited TM4SF5-mediated tumor growth in a manner that was distinct from that of the anti-tumor effect of sorafenib [30]. In addition, Kwon and colleagues reported that a mouse monoclonal antibody targeting TM4SF5 inhibited liver cancer growth [31]. TM4SF5 may, therefore, represent a novel molecular target for anti-cancer therapy, and the targeting of TM4SF5 may have certain therapeutic advantages for the treatment of advanced HCC and colorectal cancer in terms of targeting different pathways from the current therapeutics. Our results showed that Ab27 inhibited the proliferation and/or invasion of colorectal cancer cells harboring activating KRAS mutations (HCT-116 and LS174T) as well as cells harboring the KRAS wild-type (HT-29 and Colo205). These results support the possibility that Ab27 can overcome the limitations of current anti-EGFR antibodies, although this important aspect requires further investigation. It would be also worth exploring whether Ab27 is effective against cancer cells resistant to EGFR kinase inhibitors or chemotherapy. Another approach would be to investigate whether combination treatment with Ab27 and chemotherapeutic agents or targeted therapeutic agents can enhance the therapeutic benefit compared with treatment using either antibody or the drug alone in combating liver, colorectal and lung cancers.

Antitumor antibodies could be used as vehicles for the selective delivery of cytotoxic agents to tumors [32]. For example, trastuzumab emtansine (trastuzumab linked to the cytotoxic agent maytansinoids DM1) was recently approved to treat metastatic HER2-positive breast cancer. Clinical trial results showed that trastuzumab emtansine prolonged progression-free and overall survival in late-stage HER2-positive breast cancer patients who had been previously treated with trastuzumab and a taxane [33]. Considering that Ab27 binds to a cell surface receptor and is internalized to target tumor

cells, Ab27 conjugated with a cytotoxic drug could be designed and evaluated for antitumor efficacy in the future.

Ab27 is, at present, a chimeric scFv-Fc antibody. Although chimeric antibodies, such as cetuximab and rituximab, are approved for cancer treatment, Ab27 needs to be humanized to reduce immunogenicity and enhance its therapeutic efficacy. Conversion of its scFv-Fc format into a whole IgG format would increase its stability *in vivo*. The amino acid sequences of the complementary determining regions are similar between Ab27 and Ab79, and it would, therefore, be useful to generate improved/optimized antibodies from these antibodies using an affinity maturation process.

## Conclusions

We generated and evaluated two anti-TM4SF5 chimeric antibodies as potential therapeutics using *in vitro* and *in vivo* models. Ab27 efficiently recognized cell surface TM4SF5 resulting in the internalization and downregulation of TM4SF5. Ab27 inhibited the invasion and proliferation of TM4SF5-positive colon cancer and HCC cell lines, and efficiently reduced tumor growth in nude mice bearing HCC xenografts. In addition, Ab27 induced an immune cell-mediated cancer cell killing effect on TM4SF5-positive cancer cells. These results suggest that Ab27 may have potential as a therapeutic agent for the treatment of liver and colon cancers. Further studies on the functions and mechanisms of the antibody against various types of TM4SF5-positive cancers are warranted. The construction and evaluation of the humanized antibody in the context of efficacy and safety may provide important information for its future application as an anti-cancer agent.

## Abbreviations

ADCC: antibody-dependent cell-mediated cytotoxicity; EMT: epithelial-mesenchymal transition; ERK1/2: extracellular signal-regulated kinase 1/2; FAK: focal adhesion kinase; HEK293E: human embryonic kidney 293E; SD: standard deviation; siRNA: small interfering RNA; TCGA: The Cancer Genome Atlas.

## Supplementary Material

Supplementary figures.

<http://www.thno.org/v07p0594s1.pdf>

## Acknowledgments

We thank Prof. C.Y. Park (UNIST, Korea) for the Biacore 3000 system and H.J. Min for experimental assistance. This study was supported by grants from the National Research Foundation of Korea

(NRF-2016M3A9A8915731, NRF-2014R1A2A1A11049 414 and NRF-2014R1A1A2058183), and Tumor Microenvironment Global Core Research Center (GCRC; 2011-0030001), and the National Research Council of Science & Technology (NST) grant by the Korea government (MSIP) (No.CRC-15-02-KRIBB), Republic of Korea.

## Competing Interests

The authors have declared that no competing interest exists.

## References

- Forner A, Llovet JM, Bruix J. Hepatocellular carcinoma. *Lancet*. 2012; 379: 1245-55.
- Bruix J, Han KH, Gores G, Llovet JM, Mazzaferro V. Liver cancer: Approaching a personalized care. *Journal of hepatology*. 2015; 62: S144-56.
- Cunningham D, Atkin W, Lenz HJ, Lynch HT, Minsky B, Nordlinger B, et al. Colorectal cancer. *Lancet*. 2010; 375: 1030-47.
- Sala-Valdes M, Ailane N, Greco C, Rubinstein E, Boucheix C. Targeting tetraspanins in cancer. *Expert opinion on therapeutic targets*. 2012; 16: 985-97.
- Detchokul S, Williams ED, Parker MW, Frauman AG. Tetraspanins as regulators of the tumour microenvironment: implications for metastasis and therapeutic strategies. *British journal of pharmacology*. 2014; 171: 5462-90.
- Yanez-Mo M, Barreiro O, Gordon-Alonso M, Sala-Valdes M, Sanchez-Madrid F. Tetraspanin-enriched microdomains: a functional unit in cell plasma membranes. *Trends in cell biology*. 2009; 19: 434-46.
- Muller-Pillasch F, Wallrapp C, Lacher U, Friess H, Buchler M, Adler G, et al. Identification of a new tumour-associated antigen TM4SF5 and its expression in human cancer. *Gene*. 1998; 208: 25-30.
- Lee SA, Lee SY, Cho IH, Oh MA, Kang ES, Kim YB, et al. Tetraspanin TM4SF5 mediates loss of contact inhibition through epithelial-mesenchymal transition in human hepatocarcinoma. *The Journal of clinical investigation*. 2008; 118: 1354-66.
- Wu YB, Huang YS, Xu YP, Sun YF, Yu DL, Zhang XQ, et al. A high level of TM4SF5 is associated with human esophageal cancer progression and poor patient survival. *Digestive diseases and sciences*. 2013; 58: 2623-33.
- Choi S, Lee SA, Kwak TK, Kim HJ, Lee MJ, Ye SK, et al. Cooperation between integrin alpha5 and tetraspanin TM4SF5 regulates VEGF-mediated angiogenic activity. *Blood*. 2009; 113: 1845-55.
- Lee D, Na J, Ryu J, Kim HJ, Nam SH, Kang M, et al. Interaction of tetraspanin (in) TM4SF5 with CD44 promotes self-renewal and circulating capacities of hepatocarcinoma cells. *Hepatology*. 2015; 61: 1978-97.
- Lee MS, Kim HP, Kim TY, Lee JW. Gefitinib resistance of cancer cells correlated with TM4SF5-mediated epithelial-mesenchymal transition. *Biochimica et biophysica acta*. 2012; 1823: 514-23.
- Lee SA, Kim YM, Kwak TK, Kim HJ, Kim S, Ko W, et al. The extracellular loop 2 of TM4SF5 inhibits integrin alpha2 on hepatocytes under collagen type I environment. *Carcinogenesis*. 2009; 30: 1872-9.
- Lee SA, Ryu HW, Kim YM, Choi S, Lee MJ, Kwak TK, et al. Blockade of four-transmembrane L6 family member 5 (TM4SF5)-mediated tumorigenicity in hepatocytes by a synthetic chalcone derivative. *Hepatology*. 2009; 49: 1316-25.
- Jung H, Lee KP, Park SJ, Park JH, Jang YS, Choi SY, et al. Tmprss4 promotes invasion, migration and metastasis of human tumor cells by facilitating an epithelial-mesenchymal transition. *Oncogene*. 2008; 27: 2635-47.
- Berntzen G, Lunde E, Flobakk M, Andersen JT, Lauvrak V, Sandlie I. Prolonged and increased expression of soluble Fc receptors, IgG and a TCR-Ig fusion protein by transiently transfected adherent 293E cells. *Journal of immunological methods*. 2005; 298: 93-104.
- Yoon H, Song JM, Ryu CJ, Kim YG, Lee EK, Kang S, et al. An efficient strategy for cell-based antibody library selection using an integrated vector system. *BMC biotechnology*. 2012; 12: 62.
- Lee SY, Kim YT, Lee MS, Kim YB, Chung E, Kim S, et al. Focal adhesion and actin organization by a cross-talk of TM4SF5 with integrin alpha2 are regulated by serum treatment. *Experimental cell research*. 2006; 312: 2983-99.
- Nam EH, Lee Y, Moon B, Lee JW, Kim S. Twist1 and AP-1 cooperatively upregulate integrin alpha5 expression to induce invasion and the epithelial-mesenchymal transition. *Carcinogenesis*. 2015; 36: 327-37.
- Gao J, Aksoy BA, Dogrusoz U, Dresdner G, Gross B, Sumer SO, et al. Integrative analysis of complex cancer genomics and clinical profiles using the cBioPortal. *Science signaling*. 2013; 6: p11.
- Cerami E, Gao J, Dogrusoz U, Gross BE, Sumer SO, Aksoy BA, et al. The cBio cancer genomics portal: an open platform for exploring multidimensional cancer genomics data. *Cancer discovery*. 2012; 2: 401-4.
- Nimmerjahn F, Ravetch JV. Divergent immunoglobulin g subclass activity through selective Fc receptor binding. *Science*. 2005; 310: 1510-2.

23. Nahta R, Esteva FJ. Herceptin: mechanisms of action and resistance. *Cancer letters*. 2006; 232: 123-38.
24. Kim H, Jung O, Kang M, Lee MS, Jeong D, Ryu J, et al. JNK signaling activity regulates cell-cell adhesions via TM4SF5-mediated p27(Kip1) phosphorylation. *Cancer letters*. 2012; 314: 198-205.
25. Kang M, Ryu J, Lee D, Lee MS, Kim HJ, Nam SH, et al. Correlations between transmembrane 4 L6 family member 5 (TM4SF5), CD151, and CD63 in liver fibrotic phenotypes and hepatic migration and invasive capacities. *PLoS one*. 2014; 9: e102817.
26. Kang M, Jeong SJ, Park SY, Lee HJ, Kim HJ, Park KH, et al. Antagonistic regulation of transmembrane 4 L6 family member 5 attenuates fibrotic phenotypes in CCl(4)-treated mice. *The FEBS journal*. 2012; 279: 625-35.
27. Sunada H, Magun BE, Mendelsohn J, MacLeod CL. Monoclonal antibody against epidermal growth factor receptor is internalized without stimulating receptor phosphorylation. *Proceedings of the National Academy of Sciences of the United States of America*. 1986; 83: 3825-9.
28. Jaramillo ML, Leon Z, Grothe S, Paul-Roc B, Abulrob A, O'Connor McCourt M. Effect of the anti-receptor ligand-blocking 225 monoclonal antibody on EGF receptor endocytosis and sorting. *Experimental cell research*. 2006; 312: 2778-90.
29. Asghar U, Hawkes E, Cunningham D. Predictive and prognostic biomarkers for targeted therapy in metastatic colorectal cancer. *Clinical colorectal cancer*. 2010; 9: 274-81.
30. Lee SA, Lee MS, Ryu HW, Kwak TK, Kim H, Kang M, et al. Differential inhibition of transmembrane 4 L six family member 5 (TM4SF5)-mediated tumorigenesis by TSAHC and sorafenib. *Cancer biology & therapy*. 2011; 11: 330-6.
31. Kwon S, Choi KC, Kim YE, Ha YW, Kim D, Park BK, et al. Monoclonal antibody targeting of the cell surface molecule TM4SF5 inhibits the growth of hepatocellular carcinoma. *Cancer research*. 2014; 74: 3844-56.
32. Sliwkowski MX, Mellman I. Antibody therapeutics in cancer. *Science*. 2013; 341: 1192-8.
33. Verma S, Miles D, Gianni L, Krop IE, Welslau M, Baselga J, et al. Trastuzumab emtansine for HER2-positive advanced breast cancer. *The New England journal of medicine*. 2012; 367: 1783-91.